doi:10.3788/gzxb20164502.0212001

倾斜相移闭合干涉图的非迭代相位提取方法

徐建程,侯园园,陈婴
(浙江师范大学 信息光学研究所,浙江 金华 321004)

摘 要:针对带倾斜相移误差的闭合干涉图,提出一种非迭代的高精度相位提取方法.该方法用傅里叶变换估计闭合条纹的相位,并用图像分割校正相位的符号,然后利用 Zernike 多项式拟合确定倾斜相移量,最后用最小二乘拟合得到高精度相位.数值模拟结果表明:该方法的相位提取误差随着干涉图中条纹根数的增多而减小;当干涉图中条纹根数为 4.5 时,倾斜相移的估计误差为 0.37%.实验结果表明该方法的残余误差均方根值为 0.121 7rad.该方法精度高,且无需迭代计算,可应用于相移干涉测量.

关键词:相移干涉测量;条纹分析;傅里叶变换;闭合干涉图;倾斜相移误差
中图分类号:O436.1 **文献标识码**:A **文章编号**:1004-4213(2016)02-0212001-6

Non-Iterative Phase Extraction from Closed Interferograms with Tilt Shifts

XU Jian-cheng, HOU Yuan-yuan, CHEN Zhao
(*Institute of Information Optics, ZhejiangNormalUniversity, Jinhua, Zhejiang* 321004, *China*)

Abstract: A non-iterative method was proposed to extract the phase from closed interferograms with tilt-shift errors. The proposed method estimates the phase of closed interferogram by Fourier transform, corrects the sign ambiguity of phase by image segmentation, and determines the tilt-shift plane by Zernike polynomials fitting. Finally the phase is extracted accurately by least square fitting. Simulation result shows that the residual phase error of the proposed method decreases with the increasing of the number of fringes in interferograms. When the closed interferograms have 4.5 fringes, the average estimation error of tilt shift is 0.37%. Experimental result shows that the root mean square of the residual phase error is only 0.121 7 rad. The proposed method is accurate and non-iterative, can be used in phase shifting interferometry.

Key words: Phase shifting interferometry; Fringe pattern analysis; Fourier transform method; Closed interferogram; Tilt-shift error.
OCIS Codes: 120.3180; 120.2650; 120.5050; 100.2650; 070.2615

0 Introduction

Among automated interferogram analysis methods, Temporal Phase Shifting (TPS) technique is recognized as the most accurate wave-front extraction[1-2]. The measurement accuracy of the TPS depends on the errors caused by several practical limitations, including the phase shifter performance and environment instabilities. Therefore, accurate phase shift calibration procedures or self-calibrating algorithms are applied to minimize measurement errors[3-4]. Most of the published TPS algorithms assume that every pixel in an interferogram must have the same amount of phase shift relative to the first interferogram. However, due to an unbalanced piezoelectric effect in the phase shifter or instability of the optical platform, for example, some phase shifters may introduce a significant tilt. Consequently, the phase-shift values are not constants at all points but vary with a linear function across the field.

To eliminate the tilt-shift errors, on the one hand, Chen *et al*[5], Dobroiu *et al*[6] and Xu *et al*[7] proposed

Foundation item: The National Natural Science Foundation of China (No. 61205163) and Marie Curie International Incoming Fellowships (No. 301807) by the Research Executive Agency of the European Commission
First author: XU Jian-cheng (1981-), male, associate professor, Ph. D. degree, mainly focuses on information optics and phase shifting interferometry. Email: xujiancheng@zjnu.cn
Received: Aug. 18, 2015; **Accepted**: Nov. 16, 2015

some algorithms that are immune to both transitional and tilt-shift errors, however, these algorithms need intensive iterative calculations. On the other hand, methods detecting the tilt-shift errors without iterations are also studied. Patorski *et al*[8] detected the tilt-shift errors by phase shift angle histograms and lattice-site representations, but it cannot obtain the quantitative information on the tilt-shift errors. Soloviev and Vdovin[9] proposed a method that can extract the transitional values and tilt-shift errors from the difference between the fringes if the magnitude of the tilts is large. Zeng[10] proposed a method that can estimate the tilt-shift error between two interferograms by extending the regularized optical flow method. Furthermore, many algorithms[11-14] have been proposed to extract the phase from a single closed interferogram, but it is not accurate enough for high accuracy measurement because only one closed interferogram is used and the information is not enough.

To accurately extract the phase from the closed interferograms with tilt-shift errors, we use a combined spatial and temporal processing method[3]. Firstly, we determine the transitional values and tilt-shift errors from closed interferograms by Fourier-transform and then compensate for them by least squares fitting. We discuss the principles of the method, and give its verification by computer simulations and experiments.

1 Principle

1.1 Phase extraction from closed interferogram by FTM

In experimental realization, if the Piezoelectric Transducer (PZT) device of test optical element in the interferometer has orientation errors during the shift, the test surface will be tilted. In this case, the intensity at pixel (x, y) of the nth interferogram ($n=1, 2\cdots N$, $N\geqslant 3$) can be represented as

$$I_n(x,y)=A+B\cos(\varphi(x,y)+u_n x+v_n y+d_n)= A+0.5B\exp[\mathrm{i}(\varphi(x,y)+u_n x+v_n y+d_n)]+ 0.5B\exp[-\mathrm{i}(\varphi(x,y)+u_n x+v_n y+d_n)] \quad (1)$$

where I is the intensity, A is the background, B is the modulation and $\varphi(x,y)$ is the phase distribution under test. u_n and v_n denote tilt shift errors along x and y directions and d_n denotes the transitional value (piston) in the nth phase-shifted interferogram. Fig. 1(a) shows one typical closed interferogram in practical experiment. Its spectra is shown in Fig. 1(b). If Fig. 1(b) is band-pass filtered in one side of the vertical direction as shown in Fig. 1(c), its inverse Fourier transform can be written as

$$Z_{\mathrm{Re}}(x,y)+\mathrm{i}Z_{\mathrm{Im}}(x,y)= \begin{cases} 0.5B\cos[\Phi_n(x,y)]+0.5\mathrm{i}B\sin[\Phi_n(x,y)] & \text{if } \dfrac{\partial\Phi_n(x,y)}{\partial y}>0 \\ 0.5B\cos[\Phi_n(x,y)]+0.5\mathrm{i}B\sin[\Phi_n(x,y)] & \text{otherwise} \end{cases} \quad (2)$$

where $\Phi_n(x,y)=\varphi(x,y)+u_n x+v_n y+d_n$. Then the estimated phase with sign ambiguity is given by

$$\Phi_n^{\mathrm{sign}}(x,y)=\arctan\left[\frac{Z_{\mathrm{Im}}(x,y)}{Z_{\mathrm{Re}}(x,y)}\right] \quad (3)$$

Fig. 1(d) shows the estimated phase $\Phi_n^{\mathrm{sign}}(x,y)$, which has different phase signs in upper and lower parts. According to the theoretical analysis[11-13], the relation between $\Phi_n^{\mathrm{sign}}(x,y)$ and $\Phi_n(x,y)$ can be expressed as

$$\Phi_n^{\mathrm{sign}}(x,y)= \begin{cases} \Phi_n(x,y) & \text{if } \partial\Phi_n(x,y)/\partial y>0 \\ -\Phi_n(x,y) & \text{otherwise} \end{cases} \quad (4)$$

Eq. (4) shows that the real phase $\Phi_n(x,y)$ can be obtained from the estimated phase $\Phi_n^{\mathrm{sign}}(x,y)$ by correcting the phase sign in different parts.

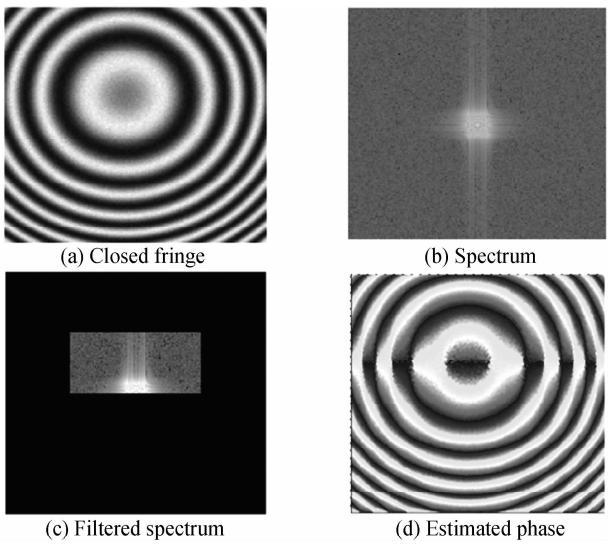

Fig. 1 Analysis of closed interferogram in frequency domain

1.2 Determination of phase sign by image segmentation

There is a visible segmentation path in Fig. 1(d), which corresponds to $\partial\Phi_n/\partial y=0$. However, it is not easy to determine the segmentation path because the estimated phase $\Phi_n^{\mathrm{sign}}(x,y)$ is wrapped and exists 2π jumps. Therefore, we firstly calculate the sine function of $\Phi_n^{\mathrm{sign}}(x,y)$ to avoid 2π jumps and the result is shown in Fig. 2(a). Secondly, we calculate the gradient of Fig. 2(a) and obtain the binary image of the gradient by setting a proper threshold. The number of segmentation points depends on the threshold used. Usually, threshold between 0.5 to 0.9 times of the maximum value is used to get enough segmentation points. Thirdly, the main segmentation points, which are discrete and locates in the place of $\partial\Phi_n/\partial y=0$, can be found easily from the binary image, and the segmentation path is obtained by linear fitting of these segmentation points, as shown in Fig. 2(b). Finally,

the sign of phase is determined and corrected according to Eq. (4) and the result is shown in Fig. 2(c). However, the obtained phase has a considerable error which is shown in Fig. 2(d). The real segmentation path will be a little different to the fitted line of these segmentation points, thus the phase error occurs near the segmentation path. By making the phase near the segmentation path has less Root Mean Square (RMS) value, the phase sign can be further corrected and the error can be partly reduced.

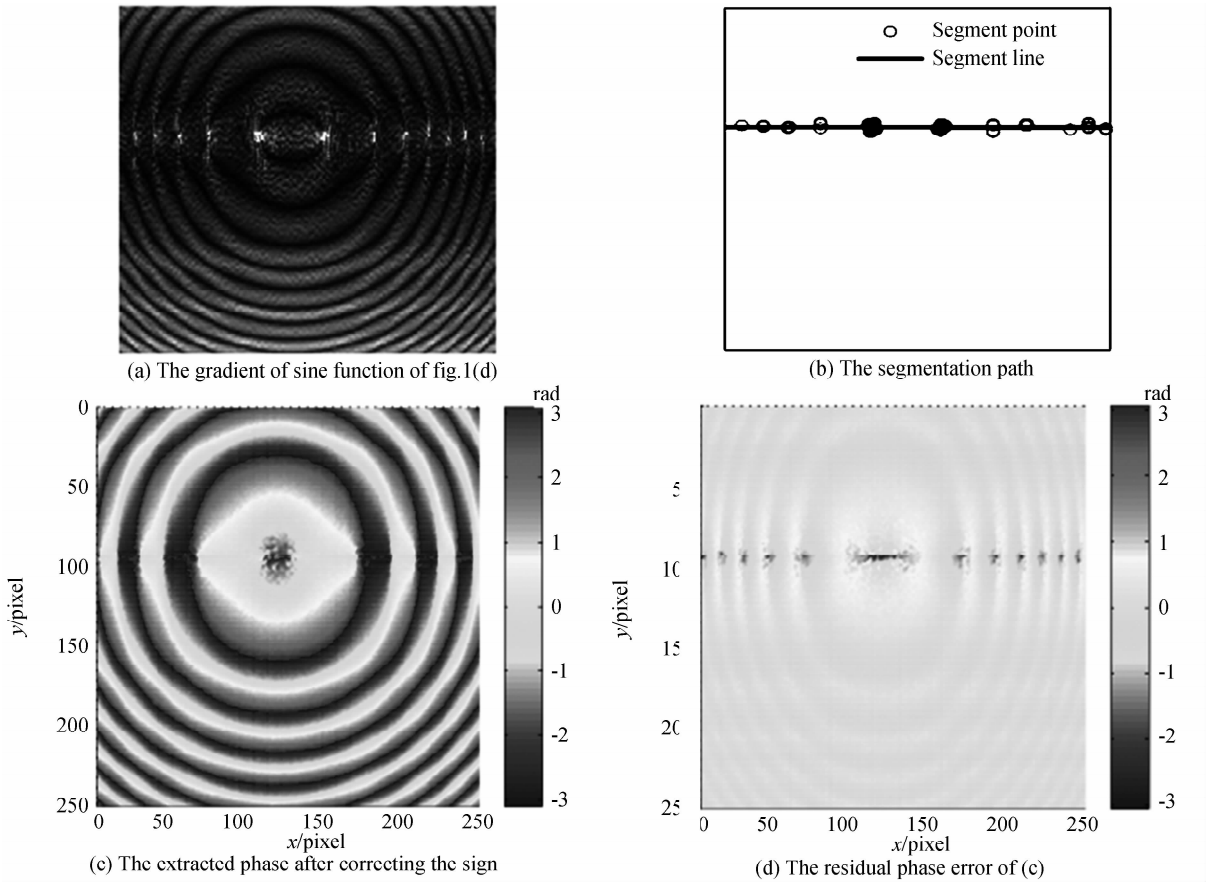

(a) The gradient of sine function of fig.1(d)
(b) The segmentation path
(c) The extracted phase after correcting the sign
(d) The residual phase error of (c)

Fig. 2 Determination of phase sign by image segmentation

1.3 Tilt-shift determination by Zernike polynomials fitting

The obtained phase $\Phi_n(x,y)=\varphi(x,y)+u_n x+v_n y+d_n$ from Section 1.2 still has local error near the segmentation path and some waviness error caused by Gibbs phenomenon in Fourier Transform Method (FTM)[11-12]. To determine the tilt-shift plane from noisy phase $\Phi_n(x,y)$, Zernike polynomials fitting method are applied over the circular or square area[16]. To improve the calculation efficiency, only 8 terms of Zernike polynomials are used. The first three terms of the Zernike polynomials mean the piston d_n, and the tilts u_n and v_n. After u_n, v_n and d_n are determined, the tilt-shift plane for the nth interferogram can be estimated as $\theta_n(x,y)=u_n x+v_n y+d_n$.

1.4 Tilt-shift compensation by least square fitting

As in the conventional phase-shifting algorithm, it is assumed that the background intensity and the modulation amplitude do not have frame-to-frame variation, i.e., they are only functions of pixels. Under the assumption, define a new set of variables as

$$\begin{cases} a(x,y)=A(x,y) \\ b(x,y)=B(x,y)\cos[\varphi(x,y)] \\ c(x,y)=-B(x,y)\sin[\varphi(x,y)] \end{cases} \tag{5}$$

For the pixel (x, y), if u_n and v_n and d_n are known, there are 3 unknowns and N equations. The unknowns can be solved by use of the over determined least-squares method if $N \geqslant 3$[3,7]. The least-squares error between theoretical and experimental interferogram $S(x,y)$ which is accumulated from all the images described by Eq. (1), can be written as

$$S(x,y)=\sum_{n=1}^{N}[I_n^{e}(x,y)-I_n^{t}(x,y)]^2 \tag{6}$$

where $I_n^{e}(x,y)$ and $I_n^{t}(x,y)$ are the experimentally measured and theoretical intensity of the interferogram. The least-squares criteria required for three unknowns ($a(x, y)$, $b(x, y)$ and $c(x, y)$) can be expressed as

$$\begin{cases}\dfrac{\partial S(x,y)}{\partial a(x,y)}=0\\ \dfrac{\partial S(x,y)}{\partial b(x,y)}=0\\ \dfrac{\partial S(x,y)}{\partial c(x,y)}=0\end{cases} \tag{7}$$

from Eq. (7) we can obtain that

$$\begin{bmatrix}a(x,y)\\ b(x,y)\\ c(x,y)\end{bmatrix}=\boldsymbol{T}\begin{bmatrix}\sum_{n=1}^{N}I_n(x,y)\\ \sum_{n=1}^{N}I_n(x,y)\cos\phi_n(x,y)\\ \sum_{n=1}^{N}I_n(x,y)\sin\phi_n(x,y)\end{bmatrix} \tag{8}$$

where

$$\boldsymbol{T}=\begin{bmatrix}N & \sum_{n=1}^{N}\cos\theta_n & \sum_{n=1}^{N}\sin\theta_n\\ \sum_{n=1}^{N}\cos\theta_n & \sum_{n=1}^{N}\cos^2\theta_n & 0.5\sum_{n=1}^{N}\sin 2\theta_n\\ \sum_{n=1}^{N}\sin\theta_n & 0.5\sum_{n=1}^{N}\sin 2\theta_n & \sum_{n=1}^{N}\sin^2\theta_n\end{bmatrix}^{-1} \tag{9}$$

From Eqs. (8)-(9), the unknowns ($a(x, y)$, $b(x, y)$, $c(x, y)$) can be solved. Then the final phase distribution can be determined as

$$\varphi(x,y)=\arctan[-c(x,y)/b(x,y)] \tag{10}$$

2 Simulations

Since it is hard to know the exact expression of an actual object surface due to many practical factors, a series of computer simulations have been carried out to verify the effectiveness of the proposed method. To check its accuracy, we define the parameters of the interferogram as follows

$$\begin{cases}\varphi(x,y)=2D\pi(x^2+y^2)\\ A(x,y)=B(x,y)=128\ \exp[-0.5(x^2+y^2)]\end{cases} \tag{11}$$

where, $0\leqslant x^2+y^2\leqslant 1$, and D means the number of fringes in interferogram. An additive white Gaussian noise with zero mean and unit variance is added to the interferogram. By assuming transitional phase shift $d=[0,0.5,1,1.5]$, and the tilts u_n and v_n are random numbers between -0.5 and 0.5, a set of four randomly tilt-shifted interferograms are generated with pixels of 300×300. One typical interferogram with 4.5 fringes ($D=4.5$) is shown in Fig. 3(a). Firstly, we extract the phase from Fig. 3(a) by FTM method (only including steps in Sections 1.1 and 1.2), and the residual phase error is shown in Fig. 3 (b), which is still considerable and cannot be ignored. The Peak-to-Valley (PV) and RMS values of Fig. 3 (b) are 4.899 8 and 0.260 7 rad, respectively. Secondly, we estimate the transitional phase shifts and the tilt-shift errors by the proposed method and the results are shown in Table 1. We do the simulation twice (case 1 and case 2). It shows that the average estimation error of the transitional phase shift and the tilt shift are 0.9% and

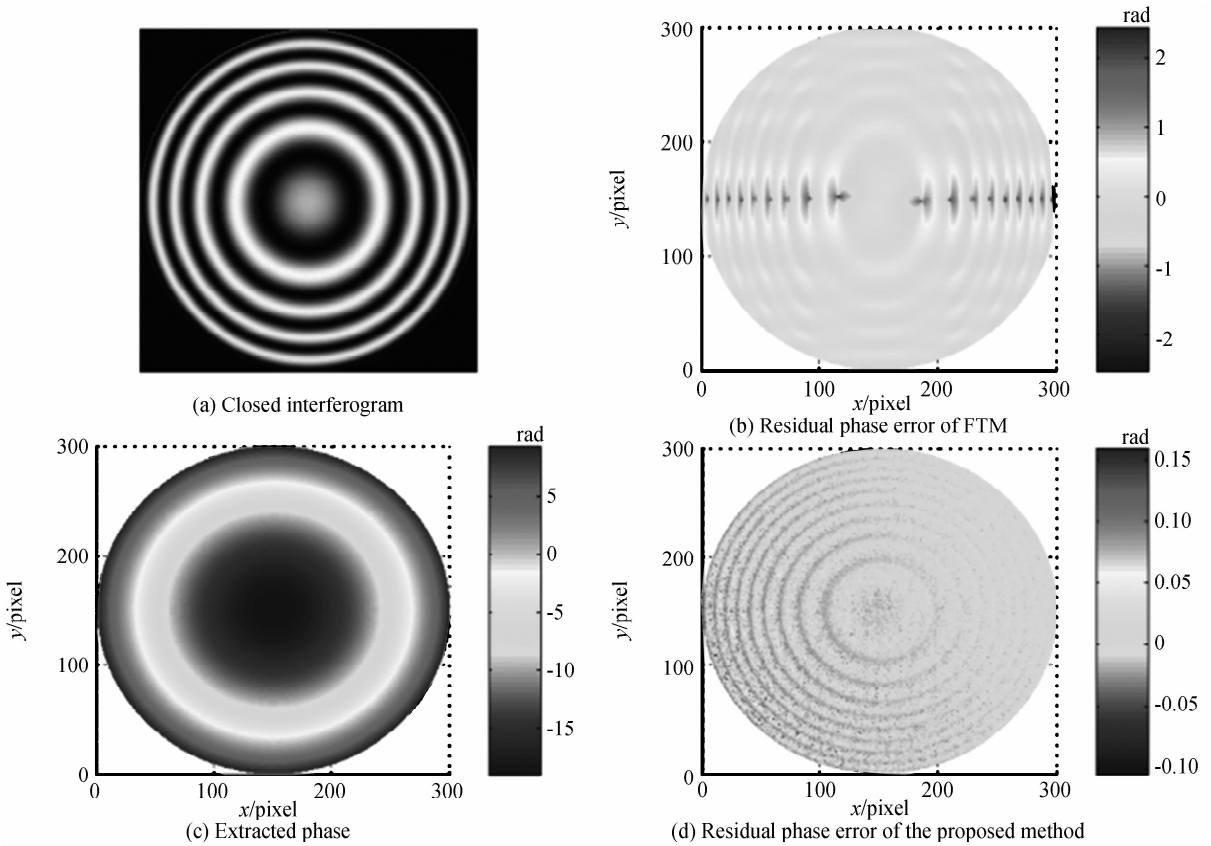

Fig. 3 Phase Extraction from closed interferograms with tilt-shift errors

0.37%. By compensating for the tilt-shift errors, the extracted phase and the residual phase error of the proposed method are obtained and shown in Figs. 3(c) and (d), respectively. The PV and RMS values of Fig. 3 (d) are 0.241 5 and 0.017 7 rad, which are less than one tenth of that for the FTM method. The reason is that the proposed method reduces the phase errors caused by the tilt-shift errors and the Gibbs phenomenon, which will exist in traditional PSI algorithms[3-4] and FTM method[11-12], respectively.

In the simulations above, we assume that the interferograms have 4.5 fringes ($D=4.5$). We also did the simulations when D between 2 and 4 and the result is shown in Table 2. Table 2 shows that the residual phase error of the proposed method decreases with the increasing of D. The residual phase error changes slowly when D between 2.5 and 4. However, it increases fast when D decreases from 2.5 to 2. It means that the proposed method works well when $D \geqslant 2.5$, but it may fail when $D<2$.

Table 1 The results of the tilt-shift estimation (unit: rad, and $d_1=u_1=v_1=0$)

	Case 1		Case 2	
	Real	Calculated	Real	Calculated
d_2	0.5	0.492 3	0.5	0.492 2
d_3	1	0.990 7	1	0.991 4
d_4	1.5	1.496 1	1.5	1.496 6
u_2	0.272 4	0.273 8	−0.147 7	−0.147 4
u_3	0.475 5	0.476 6	−0.206 1	−0.205 9
u_4	−0.213 0	−0.211 8	0.394 1	0.396 3
v_2	0.236 5	0.235 3	0.141 8	0.141 2
v_3	0.394 5	0.395 0	0.418 4	0.419 1
v_4	−0.167 1	−0.167 5	−0.383 6	−0.386 9

Table 2 Residual phase error for different numbers of fringes in interferogram (unit: rad)

Fringes	2	2.5	3	4
PV	1.096 8	0.249 5	0.246 6	0.241 8
RMS	0.275 6	0.025 3	0.019 2	0.018

3 Experiment

For further verification of the performance of the proposed method, we apply it to the practical interferograms. Fig. 4(a) shows one of four tilt-shifted closed interferograms from the QED's sub aperture stitching interferometer. The phase shifts are introduced by moving the test surface with unknown tilt-shift errors. The tilt-shift planes are determined by the proposed method and the parameters are shown as follows: the relative transitional phase steps are 0.94, 2.15 and 2.95 rad; the relative tilt-shift errors along x axis are 0.21, 0.84 and 0.74 rad and the relative tilt-shift errors along y axis are 0.33, 0.45 and 0.95 rad. By compensating for the transitional and tilt-shift errors, the measured phase is extracted by the proposed method and the result is shown in Fig. 4(b). Furthermore, the test surface is also measured by standard Zygo interferometer with vibration-isolating platform and calibrated PZT and the result is shown in Fig. 4(c), which serves as a reference distribution of the test surface. The difference between Figs. 4(b) and (c) is shown in Fig. 4 (d), which means the residual phase errors of the proposed method. Table 3 lists the PV and RMS values of Figs. 4(b)-(d). Fig. 4 shows that the phase extracted by our method is good in agreement with the reference phase. The PV and RMS values of the residual phase error are only 1.519 4 and 0.121 7 rad, respectively. It demonstrates that our method can effectively extract the phase from closed interferograms with randomly tilt-shifted errors.

Table 3 PV and RMS values of the extracted phases and the residual phase error of our method (unit: rad)

Method	Our method	PSI	Phase error
PV	17.438 1	17.690 3	1.519 4
RMS	4.434 4	4.569 5	0.121 7

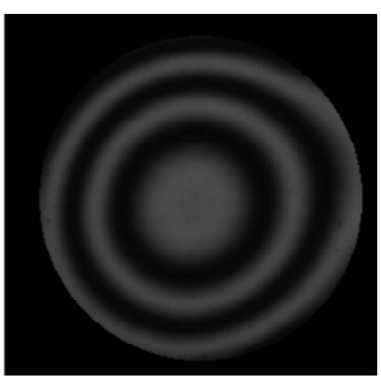

(a) Close interferogram

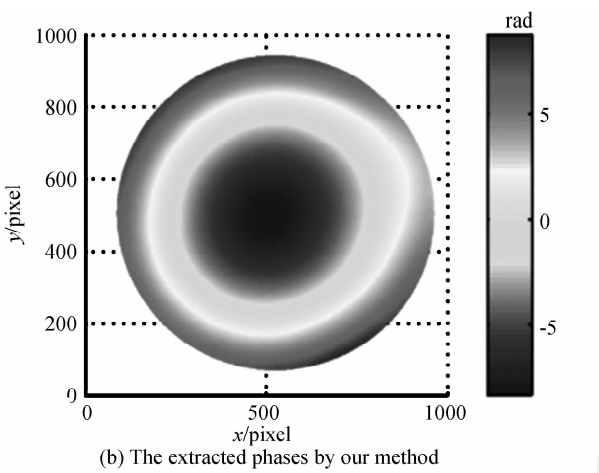

(b) The extracted phases by our method

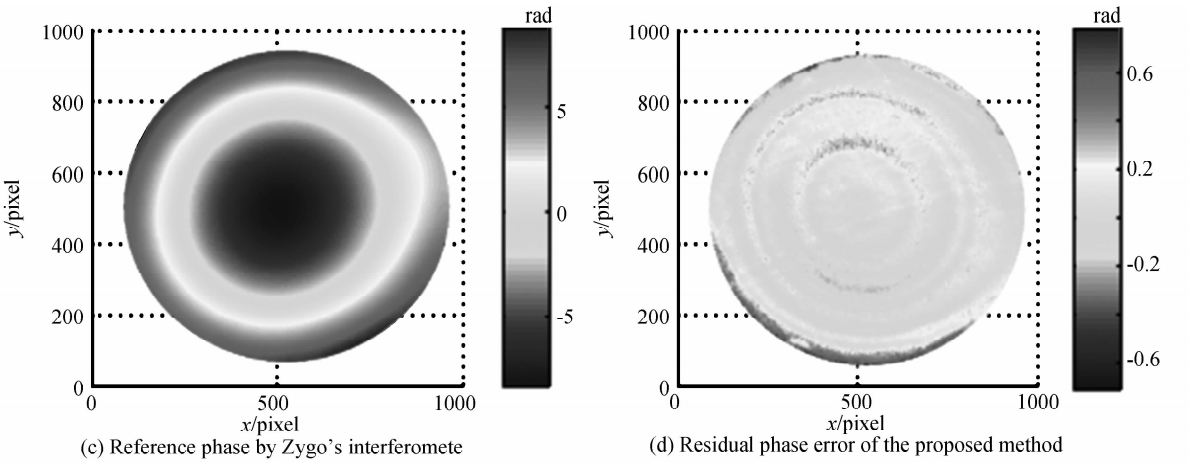

Fig. 4 Experimental results

4 Conclusion

We have proposed a combined spatial and temporal processing method to accurately extract the phase from closed interferograms with tilt-shift errors. The proposed method determines the tilt-shift errors by Fourier transform method and compensates for them by least square fitting. It is accurate and non-iterative. Simulation results show that the residual phase error of the proposed method decreases with the increasing of the number of fringes in interferograms. When the closed interferograms have 4.5 fringes, the average estimation error of the transitional phase shift and the tilt shift are 0.9% and 0.37%, and the residual phase error for the proposed method is less than one tenth of that for FTM method. Simulation and experiment results show that the proposed method accurately extracts the phase from the four randomly tilt-shifted closed interferograms with more than 2.5 fringes. The method will be useful in precision metrology.

Reference

[1] LIU F, WU Y, WU F. Phase shifting interferometry from two normalized interferograms with random tilt phase-shift [J]. *Optics Express*, 2015, **23**(15): 19932-19946.

[2] XU J, JIN W, CHAI L, *et al*. Phase extraction from randomly phase-shifted interferograms by combining principal component analysis and least squares method [J]. *Optics Express*, 2011, **19**(21): 20483-20492.

[3] GOLDBER K A, BOKOR J. Fourier-transform method of phase-shift determination[J]. *Applied Optics*, 2001, **40**(17): 2886-2894.

[4] WANG Z, HAN B. Advanced iterative algorithm for phase extraction of randomly phase-shifted interferograms[J]. *Optics Letters*, 2004, **29**(14): 1671-1673.

[5] CHEN M, GUO H, WEI C. Algorithm immune to tilt phase-shifting error for phase-shifting interferometers[J]. *Applied Optics*, 2000, **39**(32): 3894-3898.

[6] DOBROIU A, APOSTOL A, NASCOV V, *et al*. Tilt-compensating algorithm for phase-shift Interferometry [J]. *Applied Optics*, 2002, **41**(13): 2435-2439.

[7] XU J, XU Q, CHAI L. Iterative algorithm for phase extraction from interferograms with random and spatially nonuniform phase shifts [J]. *Applied Optics*, 2008, **47**(3): 480-485.

[8] PATORSKI K, STYK A, BRUNO L, *et al*. Tilt-shift error detection in phase-shifting interferometry [J]. *Optics Express*, 2006, **14**(12): 5232-5249.

[9] SOLOVIEV O, VDOVIN G. Phase extraction from three and more interferograms registered with different unknown wavefront tilts [J]. *Optics Express*, 2005, **13**(10): 3743-3753.

[10] ZENG F, TAN Q, GU H, *et al*. Phase extraction from interferograms with unknown tilt phase shifts based on a regularized optical flow method[J]. *Optics Express*, 2013, **21**(14): 17234-17248.

[11] XU Jian-cheng, CHEN Zhao. Phase demodulation of single closed interferogram based on Fourier transform [J]. *Acta Photonica Sinica*, 2014, **43**(8): 0810001.

[12] LI B, CHEN L, BIAN J, *et al*. A demodulation method for the circular carrier interferogram using phase stitching [J]. *Optics and Lasers in Engineering*, 2011, **49**(9): 1118-1123.

[13] JESUS M, FRANCISCO J C, MIGUEL M, *et al*. Phase recovery from a single interferogram with closed fringes by phase unwrapping[J]. *Applied Optics*, 2011, **50**(1): 22-27.

[14] QIAN K, SEAH H. Sequential demodulation of a single fringe pattern guided by local frequencies [J]. *Optics Letters*, 2007, **32**(2): 127-129.

[15] LI Meng-yang, LI Da-hai, WANG Qiong-hua, *et al*. Wavefront reconstruction with orthonormal polynomials in a square area[J]. *Chinese Journal of Lasers*, 2012, **39**(11): 1108011.